Cell Volume Measurement Using Scanning Ion Conductance Microscopy

Yuri E. Korchev,* Julia Gorelik,* Max J. Lab,† Elena V. Sviderskaya,‡ Caroline L. Johnston,* Charles R. Coombes,* Igor Vodyanoy,†§ and Christopher R. W. Edwards*

*Division of Medicine, Imperial College School of Medicine, Medical Research Council Clinical Sciences Centre, Hammersmith Campus, Du Cane Road, London W12 0NN, †Division of National Heart and Lung Institute, Imperial College School of Medicine, Charing Cross Campus, St. Dunstan's Road, London W6 8RP, ‡Department of Anatomy and Developmental Biology, St. George's Hospital Medical School (University of London), Cranmer Terrace, London SW17 0RE, and §Office of Naval Research International Field Office, 223 Old Marylebone Road, London NW1 5TH, United Kingdom

ABSTRACT We report a novel scanning ion conductance microscopy (SICM) technique for assessing the volume of living cells, which allows quantitative, high-resolution characterization of dynamic changes in cell volume while retaining the cell functionality. The technique can measure a wide range of volumes from 10^{-19} to 10^{-9} liter. The cell volume, as well as the volume of small cellular structures such as lamelopodia, dendrites, processes, or microvilli, can be measured with the 2.5×10^{-20} liter resolution. The sample does not require any preliminary preparation before cell volume measurement. Both cell volume and surface characteristics can be simultaneously and continuously assessed during relatively long experiments. The SICM method can also be used for rapid estimation of the changes in cell volume. These are important when monitoring the cell responses to different physiological stimuli.

INTRODUCTION

Regulation of cell volume is a fundamental cellular homeostatic mechanism. Most cells are able to regulate their volume. Normal cellular functions, such as secretion, ion transport (the movement of ions is followed by a corresponding movement of water), and a cell's adaptation to a changing osmotic environment, often require complex reorganization of cell shape and volume (Hallows et al., 1991; Swanson et al., 1991; Hoffmann et al., 1993; Alvarez-Leefmans et al., 1994; Valverde et al., 1996). To investigate the physiology and pathology associated with cell volume regulation, it is important to use an appropriate technique that allows quantitative, high-resolution characterization of cell volume while retaining the cell functionality. Currently, there are two major approaches to assess cell volume. First, one that permits measurements of relative changes in cell volume, and a second, that allows actual measurements of cell volume. The most commonly used techniques of the first approach are based on continuous monitoring of the intracellular concentration of loaded reagents (fluorescent dyes or ions). The concentration of these intracellular markers depends on the amount of cell water, and thus changes when cell water volume is altered. Thus, by continuous monitoring of the intracellular concentration of these reagents/ions using quantitative fluorescence microscopy (Lee, 1989; Crowe et al., 1995) or ion-sensitive microelectrodes (Alvarez-Leefmans et al., 1992), the relative changes in cell water volume can be measured. In some experimental condition, the relative changes in cell volume can be assessed by a simple electrophysiological method for continuous measurement of cell height (Kawahara et al., 1994). The method is well suited for studying cell volume in cell monolayers where cell expansion is mainly possible in the vertical direction. In this method, a tip of a glass micropipette is placed on the cell surface so that ion flow to the micropipette is partially restricted. Any changes in cell volume induce changes in cell height that consequently influence ion flow. Registering changes in ion flow allows estimation of changes in cell height and volume.

The second approach for investigating cell volume includes methods that allow actual measurements of cell volume. Impedance and light-microscopy are commonly used methods. The impedance method allows fast estimation of volume of a large number of cells (e.g., Nakahari et al., 1990). However, the technique is limited to certain experimental conditions, because it is only applicable to cells of nearly spherical shape in suspension. Light microscopy methods, such as video-enhanced contrast optical microscopy (Nakahari et al., 1990), light microscopy with spatial filtering (Farinas et al., 1997), and laser light-scattering system (McManus et al., 1993) have been used to estimate cell shape and, consequently, cell volume. Some optical microscopy methods have a good temporal resolution, and changes in cell volume can be estimated in submillisecond scale (e.g., Meinild et al., 1998). However, generally, these methods have limited spatial resolution, and the cell plasma membrane cannot always be clearly visualized. Currently, one of the most advanced ways of estimating cell volume is by scanning laser confocal microscopy (SLCM). Image sets consisting of very thin, serial optical sections across the cell can be obtained and a three-dimensional model of an individual cell constructed using digital image processing techniques (Guilak, 1994; Zhu et al., 1994; Errington et al., 1997). However, even this method

Received for publication 24 May 1999 and in final form 13 October 1999.

Address reprint requests to Yuri E. Korchev, Division of Medicine, Imperial College School of Medicine, Hammersmith Campus, 5th Flr. MRC Clinical Sciences Centre, Du Cane Road, London W12 0NN, U.K. Tel.: +44-181-383-2362; Fax: +44-181-383-8306; E-mail: y.korchev@ic.ac.uk.

0006-3495/00/01/451/07 $2.00

has limitations. Photodynamic damage to the biological sample remains a serious problem of SLCM (e.g., Saito et al., 1998). Special requirements are needed for specimen preparation. Sample transparency or specific experimental conditions when cell growth requires a special substrate (e.g., a membrane filter) can limit SLCM resolution. The method becomes more convoluted when long-duration observations of living cell shapes are necessary.

New techniques, such as scanning probe microscopy (SPM) (Binnig and Rohrer, 1982; Binnig et al., 1986; Hansma et al., 1989; Bard et al., 1991), have showed great potential for studying different samples, in some cases with atomic resolution. They also have proved to be capable of producing high-resolution images of biological samples and cell surfaces and providing important information on their functions (Arkawa et al., 1992; Hansma and Hoh, 1994; Henderson et al., 1992; Radmacher et al., 1992; Schoenenberger and Hoh, 1994). New generations of SPM will provide ever-improving tools to study biological samples. One of these, scanning ion conductance microscopy (SICM), is capable of high-resolution imaging of living cells, and direct visualization of changes in cell architecture (Korchev et al., 1997a,b). We now report a new SICM technique for assessing cell volume, including the volume of membrane surface protrusions.

METHODS

Imaging system

A scanning ion conductance microscope

The sensitive probe of the SICM is a glass micropipette filled with electrolyte, which is connected to a high-impedance, head-stage current amplifier and mounted on a computer-controlled three-axis translation stage. The control electronics drive the translation stage to scan the specimen under the micropipette probe. The probe tip's position, in relation to the sample surface, strongly influences the ion current through the pipette—the ion current declines as the tip–sample separation diminishes. The ion current provides a signal for the feedback loop, which controls the vertical axis of the positioning system and ensures that the sample and probe do not make contact. To scan the sample, we have used a three-axis piezo translation stage (Tritor 100, Piezosystem, Jena, Germany) with 100-μm travel distance in x, y, and z directions. As a piezo driver, we have used a high-voltage amplifier with high current output (System ENV 150, Piezosystem). The control/data acquisition hardware and software are produced by East Coast Scientific (Cambridge, England). The electronics consist of a decoder, four digital-to-analog converters, and two analog-to-digital converters. The DSP card (DSP32C PC, Loughborough Sound Images plc, Loughborough, England) of a PC functions as a front-end controller and provides digital feedback and scan control. The basic arrangement of the SICM was described elsewhere (Korchev et al., 1997b).

The micropipettes were made from 1.00 mm outer diameter, 0.58 mm inner diameter glass microcapillaries (Clark Reading, Electromedical Instruments, UK) on a laser-based Brown–Flaming puller (model P-2000, Sutter Instrument Company, San Rafael, CA). We estimated the tip radius of the micropipettes used in the present series of experiments to be ~50 nm, and the cone angle of the tip to be ~1.5° (scanning electron microscopy data not shown). The micropipettes and the bath were filled with the same solutions, usually physiological or growth media. The measured micropipette resistance was usually ~500 MΩ. The samples were usually placed on petri dishes, glass coverslips, or membrane filters and imaged in the appropriate medium.

Cell volume calculation

Previously, we have demonstrated that SICM is extremely well suited for imaging living cell surfaces in physiological or growth media (Korchev et al., 1997a). Cell imaging with SICM involves raster scanning. That is, the SICM image consists of a three-dimensional map of the apical cell surface with a limited number of points, n, where each raster scan point represents a cell height. Before assessing cell volume using the SICM, we have to measure the vertical position (Z_{REF}) of the probe tip on the substrate where cells were grown (Fig. 1 *A*). This allows us to calculate the real cell height $z(x, y)$ by subtracting Z_{REF} from the measured height value ($Z_{(x,y)}$). This is especially important when imaging a cluster of cells, and the acquired image does not include a reference point to the substrate. Assuming that basal cell membrane has a close contact with the substrate (e.g., glass coverslip, porous membrane) a cell volume (V_{Cell}) can be estimated by

$$V_{Cell} = \sum_{1}^{n} z(x, y) \times dx \times dy, \quad (1)$$

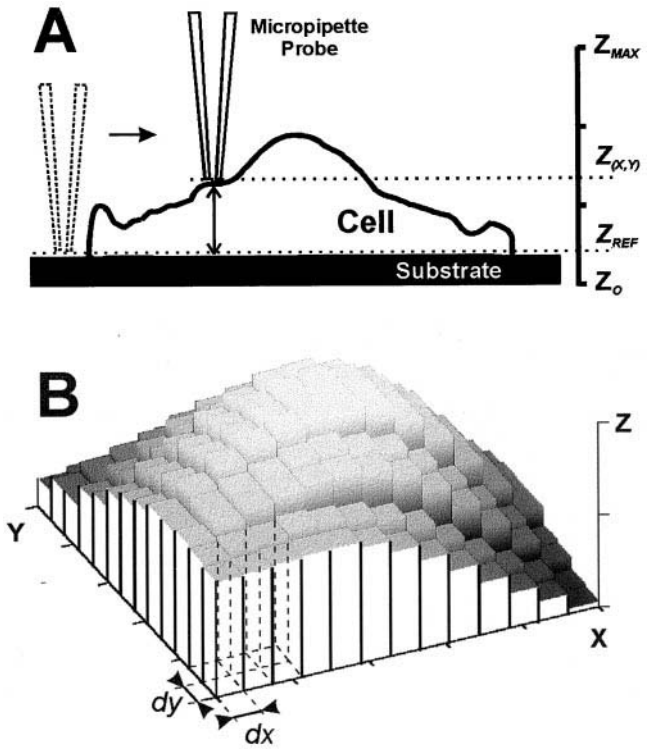

FIGURE 1 (*A*) Cell height and (*B*) volume measurements using SICM. (*A*) Z_{MAX}–Z_0 is a maximum vertical displacement range of the SICM piezoelectric translation stage. The maximum range of our SICM is 100 μ. Z_{REF} is a vertical position of the micropipette probe on the substrate surface and $Z_{(X,Y)}$–Z_{REF} is a cell height at X and Y coordinate. (*B*) The three-dimensional topographical image (250-nm width and 50-nm height) of 13 × 13 raster scan points extracted from a SICM data set. The volume under the surface can be determined by the sum of the volume of rectangular prisms, with given width dx and length dy of raster scan increments, and the height $z(x, y)$, which is equal to the cell height at each raster scan point.

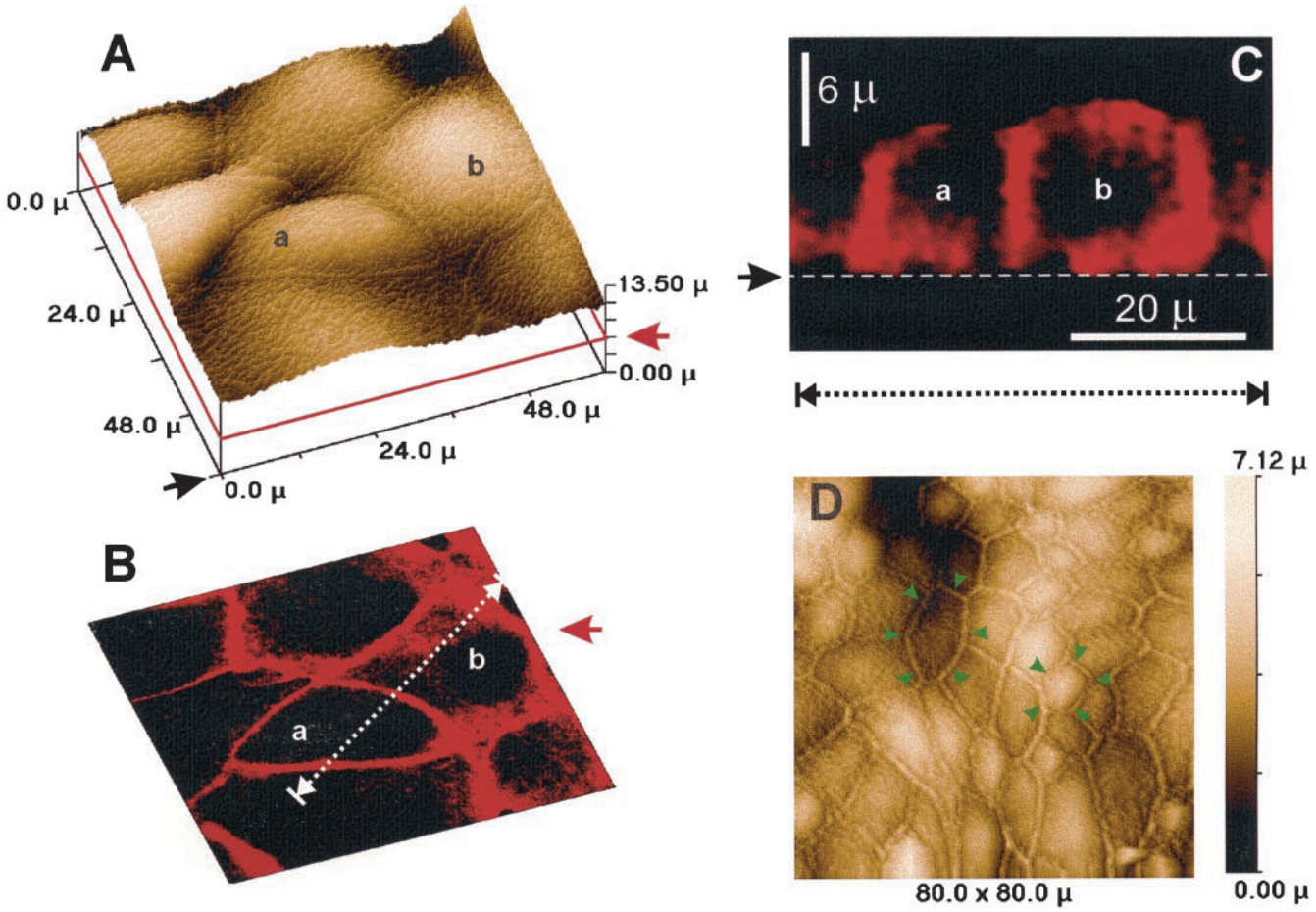

FIGURE 2 The scanning ion conductance and scanning laser confocal microscopy images of A6 cells. (*A*) The SICM image of a fixed cell monolayer grown on the glass coverslip. The coverslip surface position is marked by the black arrow and corresponds to 0.0 μ. The red arrow indicates the vertical position of the acquired SLCM for the section in (*B*). (*B* and *C*) The SLCM images of the same cell monolayer stained with rhodamin-phalloidin (at the red arrow indicated in panel *A*), i.e., vertical position of the SLCM section. Panel *C* represents the vertical SLCM section across two cells (marked a and b in both Panels *A* and *B*). The lateral position is indicated by the dotted white diagonal double-headed arrow line in panel *B*. (*D*) The SICM image of living A6 cells growing on the membrane filter. The color bar at the right represents the relative cell height. To obtain the real cell height, the 25.6-μ length to the substrate (Z_{REF}) should be added to the relative cell height value.

where n is a number of scan points per cell, $z(x, y)$ is the cell height at each raster scan point, dx and dy are scan increments (pixel size) in x and y directions (Fig. 1 *B*). The current SICM has a 10-nm vertical and 50-nm lateral resolution. This allows an estimate of the volume with a 2.5×10^{-5} μ^3 (2.5×10^{-20} liter) resolution. The $z(x, y)$ and V_{Cell} values can be assessed with less than 0.2% error.

Calculation of surface characteristics

The cell surface area (S_{Cell}) can be calculated as a sum of areas ($S_{Triangle}$) of each triangle formed on the cell surface with coordinates of three adjacent SICM scan points,

$$S_{Cell} = \sum_{1}^{n-2} S_{Triangle}, \qquad (2)$$

where n is a number of raster scan points obtained within the cell surface.

Cell roughness can be estimated as a root average of square differences in cell height. That is, expressed as RMS,

$$RMS = \left[\left(\frac{1}{n}\right) \times \sum_{i=1}^{n} (z_i - Z_{AV})^2\right]^{1/2}, \qquad (3)$$

where n is a number of scan points, z_i is a cell height at each raster scan point and Z_{AV} is an average cell height.

The current SICM routings allows a 4.5×10^{-3} μ^2 resolution for S_{Cell} and a 10^{-2} μ resolution for RMS measurements.

Scanning laser confocal microscopy

To verify the SICM method of volume measurement, the following additional modifications were introduced to our existing SICM optical system (Korchev et al., 1997a,b) to enable simultaneous laser confocal microscopy/SICM imaging of the same specimen. The current control/data acquisition hardware and software (East Coast Scientific, Cambridge, En-

gland) and the piezo-control system (Piezosystem) were used to scan the specimen under the micropipette tip, or to perform confocal microscopy scanning. The mechanical and piezoelectric translation stages (Tritor, Piezosystem) were added to the SICM for coordinating optical and topographical imaging of the same area. The excitation light source was provided by an LCM-F-6c laser diode (473-nm wavelength, Laser Compact, Moscow, Russia) and a GPNT-02 laser diode (532-nm wavelength, Lasertechnik, Bremen, Germany). The optical recording system consisted of a Nikon Diaphot inverted microscope (Diaphot 200, Nikon Corporation, Tokyo, Japan) equipped with oil-immersion objective lOOX 1.3 NA, an epi-fluorescent filter block, and a photomultiplier with a pinhole (D-104–814, Photon Technology International, Surbiton, England).

The cell volume was estimated from a data set of thin serial SLCM optical sections using digital image processing techniques described elsewhere (Guilak, 1994; Zhu et al., 1994; Errington et al., 1997). Relative changes in cell volume were assessed using fluorescence methods described in detail elsewhere (Crowe et al., 1995).

Cell preparation

Renal tubular cells, A6 cell line

A single A6 cell line in the 117th passage derived from *Xenopus laevis* renal tubular cells was kindly provided by Dr. DeSmet (Belgium). All experiments were carried out between the 120th and 123rd passages. Cells were cultured as described previously (Sariban-Sohraby et al., 1984) on glass coverslips or on membrane filters (Falcon, Bedford, MA). Cells were grown and kept in a medium of a mixture of part modified Ham's F-12 and part Leibovitz's L-15, modified to contain 105 mM NaCl and 25mM $NaHCO_3$ (Gibco, Paisley, UK). The mixture was supplemented with 10% fetal calf serum (Gibco), 1% streptomycin, 1% penicillin (Gibco). Cells were maintained at 28°C in an atmosphere of humidified air plus 1% CO_2. Cells were passaged and used between days 3 and 4 when they were 80–90% confluent. Aldosterone (Sigma, Dorset, UK) was added in a concentration of 1.5 μM. For staining of actin cytoskeleton, A6 cells were fixed using 4% formalin (Sigma) in phosphate-buffered saline (PBS) for 10 min, followed by 0.1% Triton X-100 (Sigma) extraction for 5 min, rewashed three times with PBS and then stained by Rhodamin-phalloidin (Sigma) (1:1000) 15 min at 37°C.

Ventricular myocytes

Ventricular myocytes were isolated from the hearts of 1- to 2-day-old rats after Iwaki et al. (1990). Cells were kept in a DMEM medium (Gibco) with 15% fetal calf serum (Gibco), 1% streptomycin, 1% penicillin (Gibco), 1% NEAA (Gibco). 100 μg/ml G418 geniticin (Gibco) was added for inhibiting of fibroblast growth. Cells were maintained at 37°C, in an atmosphere of humidified air plus 5% CO_2. Cells were used after 2 days after plating. Myocytes were cultured on glass coverslips. For fluorescent recording, they were stained with acridine orange/ethidium bromide AM (Sigma) (1:100) for 20 min at 37°C in a medium containing a mixture of part Leibovitz's L-15 (Gibco) and part buffer (115 mM NaCl, 5 mM KCl, 0.8 mM $MgSO_4$, 1.2 mM $CaCl_2$, 10 mM Hepes (Sigma)—pH7.4, rewashed five times with the medium.

T47D breast cancer cells

The T47D cell line was originally isolated from the pleural effusion of a 54-year-old woman with ductal carcinoma of the breast. Cells were cultured in RPMI 1640 (Sigma) supplemented with 10% FCS (Sigma), 100 μg/ml streptomycin, 100 units/ml penicillin, and 2 mM glutamine (Sigma) and were maintained at 37°C in a humidified atmosphere containing 5% CO_2. For use in experiments, cells were plated onto glass coverslips, grown in serum free RPMI 1640 for 24 h and stimulated with 30ng/ml FGF2.

RESULTS AND DISCUSSION

Whole cell volume

We have used SICM to estimate the volume of single cells in a cell monolayer. The kidney epithelial cell line A6 was grown on a glass coverslip until the cells attained a dense monolayer. Because SICM allows imaging both of fixed and of living cells, in this particular experiment, the cells were fixed with 4% formaldehyde to abolish any cellular dynamics for subsequent imaging by scanning confocal microscopy. Thereafter, the cells were imaged with the SICM (Fig. 2 *A*). The cell boundaries are clearly marked with denser microvilli. Because the cell boundaries are easily visible, the cell volume of a single cell or a scanned cell monolayer can be calculated using Eq. 1 assuming that cells are closely attached to the substrate. The calculated volume of a 60 $\times$ 60 μ area of cell monolayer (Fig. 2 *A*) is equal to 36,637 μ^3. The volume of the cells marked a and b is 4667 and 7171 μ^3, respectively. The cell volume was also assessed using scanning confocal microscopy (Guilak, 1994; Zhu et al., 1994; Errington et al., 1997). We used a set of very thin serial optical slices, similar to those shown in

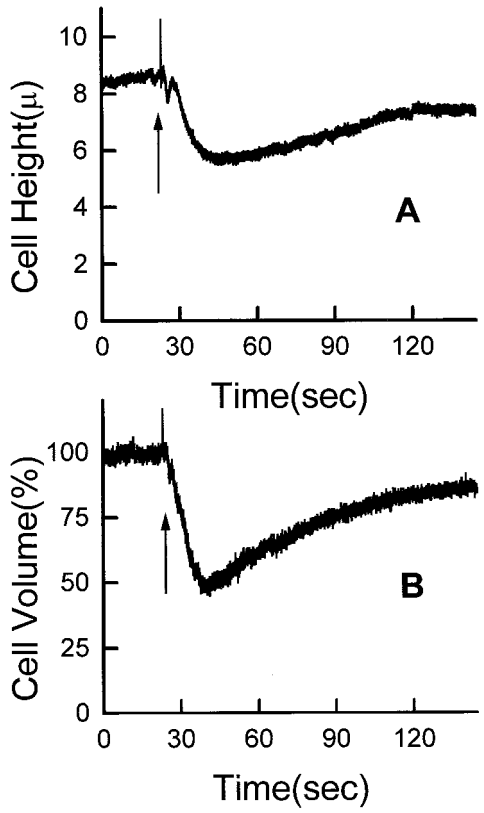

FIGURE 3 Osmotically induced (*A*) height and (*B*) volume changes in single cultured cardiac myocyte. Osmotic stress was induced by increasing NaCl concentration (240 mM) in the cell growth medium (*vertical arrows*). (*B*) Cells were loaded with a fluorescent dye and relative changes in cell volume were recorded as described elsewhere (Lee, 1989). (*A*) At the same time the changes in cell height were registered by SICM.

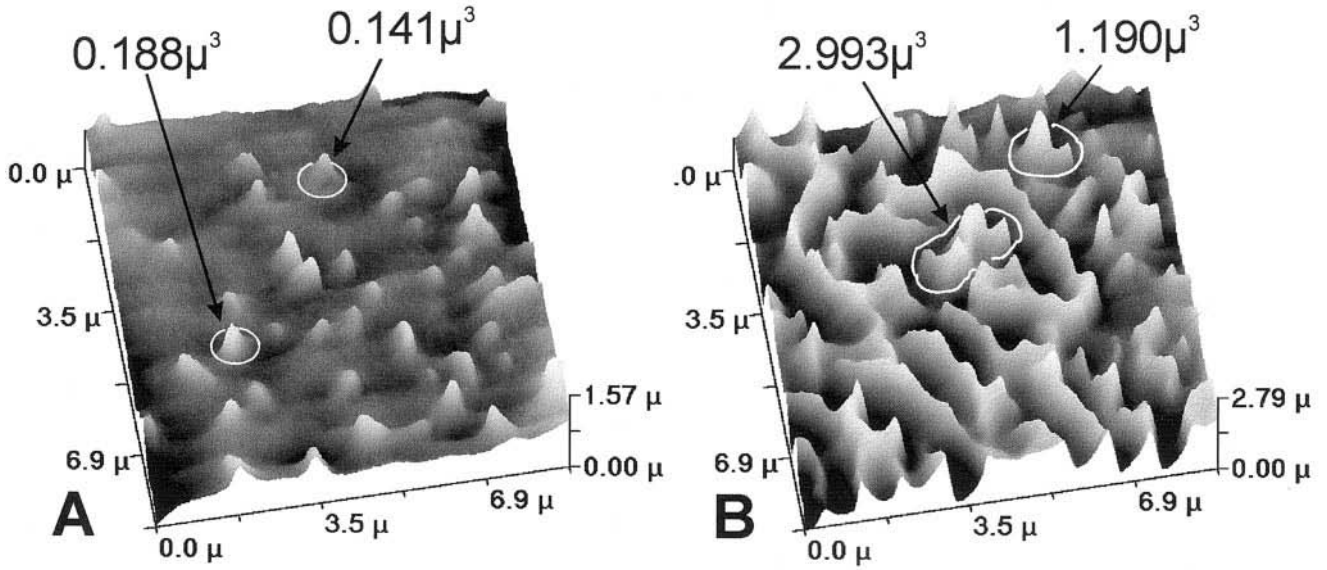

FIGURE 4 SICM images of a small area of A6 cells. Panels *A* and *B* show the differences in microvilli structure in the cells during differentiation. Cells were plated on petri dishes and imaged in growth medium.

Fig. 2, *B* or *C* across the same cells scanned by the SICM (Fig. 2 *A*) to confirm these calculations. Using digital image processing, the shape of the cell monolayer was reconstructed, and cell volume was estimated as 37,500 μ^3 for the scanned cell monolayer, and 5100 and 7600 μ^3 for cells a and b (Fig. 2 *B*), respectively. The cellular volumes estimated by these two methods are comparable, validating the SICM technique for volume measurement. The assumption that cells are closely attached to the substrate is supported by confocal microscopy data. Fig. 2 *C* illustrates a vertical slice across the cell monolayer at the position indicated by the diagonal dotted double arrowhead on the image in Fig. 2 *B*. The epithelial cells are attached to the substrate surface indicated by a white horizontal dotted line in *Panel C*, and that the cell–cell contacts are arranged perpendicular to the substrate (Fig. 2 *C*). Furthermore, the horizontal optical slice across the middle of the cell monolayer (indicated by the red arrows in Figs. 2, *A* and *B*) shows the lateral location of cell boundaries (Fig. 2 *B*) that closely matches the position of cell borders marked as denser microvilli on the cell surfaces in the SICM image (Fig. 2 *A*). Cell heights of ~3 μ assessed by scanning confocal microscopy are also similar to those (~12 μ) measured by SICM (see vertical scale in Fig. 2 *A*).

The SICM method has several advantages over the scanning confocal microscopy approach. It has a higher spatial resolution—50-nm lateral and 10-nm vertical resolution, compared with about 250- and 1000-nm resolution of scanning confocal microscopy under optimal conditions. The SICM technique does not induce photo damage to the biological sample (compare with SLCM, e.g., Saito et al., 1998) and does not require any preliminary preparation or staining of cells before imaging. The transparency of the sample, or the focal length of the objective, does not limit the SICM routines. The latter is important when the cells are grown on a special material such as permeable polymeric films, and when different growth mediums are required to bathe the apical and basal sides of the cell monolayer. Figure 2 *D* illustrates the SICM image of living A6 cells growing on a membrane filter. The volume of any imaged cell can be easily estimated. For example, the volume of individual cells marked by green arrows in Fig. 2 *D* is 3569 μ^3 (*left cell*) and 2119 μ^3 (*right cell*).

Rapid estimation of volume

The SICM method can also be used for rapid estimation of the changes in cell volume by measuring dynamic changes in cell height with a 5×10^{-3}-s temporal resolution. This is extremely well suited for studying growing monolayers where cell expansion is mainly in the vertical direction. The volume of an isolated cell can also be estimated by this approach in conjunction with light microscopy measurement of lateral cell dimensions. Figure 3 *A* shows single-cell height changes (SICM data) as a result of osmotic stress. In this experiment, a hypertonic solution was applied to a single cardiac myocyte. Osmotic stress induced a 33% reduction in cell height without any significant changes in cell length (light microscopy observation). The last is probably due to the strong attachment of the cell to the substrate. Considering a cylindrical shape and no length change of the myocyte, by calculation, the 33% reduction in cell height (diameter) gives a 55% decrease in cell volume. Figure 3 *B* also shows the simultaneous measurements of the relative cell volume changes (fluorescence measurements). These

relative changes in cell volume were assessed using fluorescence methods described in detail elsewhere (Crowe et al., 1995). Osmotic stress induced a 52% reduction in cell volume. The cell volume changes are comparable as assessed by both methods.

Changes in local cell volume and cell roughness

Dynamic changes of cellular volume are invariably accompanied by a complex rearrangement of cell shape. The SICM can provide important structural information allowing detailed quantitative analysis of highly local changes in cell volume. Volume, as well as surface characteristics of small cellular structures such as lamelopodias, dendrites, processes, or even microvilli, can be precisely measured. Figure 4 illustrates the development of microvilli on an A6 cell surface. During differentiation, A6 cells form a tight monolayer and increasing numbers of microvillus structures protrude through the apical cell membrane (compare Fig. 4, *A* and *B*). The volume of a single microvillus increases more than 10 times (0.141 and 0.188 μ^3 in *Panel A* increasing to 1.190 and 2.993 μ^3 in *Panel B*). Importantly, the volume of a single microvillus can be assessed with a resolution better than 0.1 femtoliter and less than 5% error. The volumes of all the microvilli in *A* (7.190 μ^3) rises more than 10-fold compared to that in *B* (95.554 μ^3).

Cell volume changes are often accompanied by complex reorganization of cell surfaces, which are important in cell volume regulation. The SICM method can provide quantitative characterization of the cell surfaces. For example, cell surface area, and ruggedness characteristics can be estimated. If we compare the two SICM images in Fig. 4, *A* and *B*, the cell membrane ruggedness or roughness (expressed as RMS) increases by 3.67 times from 0.116 to 0.426 μ, and the apical cell surface area S_{Cell} by 2.40 times, from 90 to 217 μ^2 per scanned region.

Moreover, both volume and surface characteristics can be simultaneously and continuously assessed during relatively long experiments. This could be important when monitoring the effects on cell dynamics of physiological, pharmacological, or molecular interventions. For example, we know that growth factor treatment of cells activate signal transduction cascades leading to changes in cell morphology, motility, and mitogenesis (Basilico and Moscatelli, 1992). Figure 5 illustrates the effect of FGF2 on T47D cell surface characteristics and cell volume. After addition of FGF2, the microvillus structures start to protrude through the cell membrane (Fig. 5 *B*) significantly increasing relative cell surface roughness (Fig. 5 *A*). This result correlates with previous observations of increased polymerization of actin at the periphery of the cell-forming protruding membrane ruffles after treatment of T47D cells with FGF2 (Johnston et al., 1995). Both changes in F-actin organization and increase of microvillus density are observed 10 min after addition of FGF2. Two hours after addition of FGF2, the breast cancer

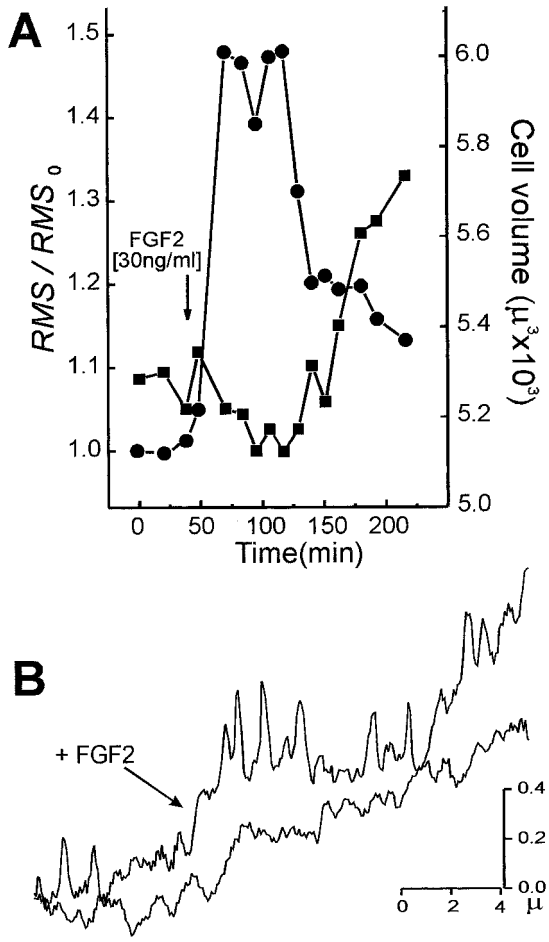

FIGURE 5 (*A*) FGF2-induced volume (–■–) and membrane roughness (–●–) changes in the breast cancer cell (T47D cell line) measured by SICM. The vertical arrow indicates the addition of FGF2. Membrane roughness is expressed as RMS normalized to its initial value (RMS_0 at 0 time). (*B*) Two single profiles across a breast cancer cell surface obtained at the same position before and after 2 h of FGF2 treatment.

cells display an increase in cell volume and a decrease in cell surface roughness (Fig. 5 *A*). The decrease in cell surface roughness could be explained by stretching of the cell membrane during cell volume increase. These observations may lead to clarification of how a cell can preserve its integrity during volume changes to maintain its functionality.

Summary

The SICM method has several advantages over currently used techniques for the measurement of cell volume. First, it has a high resolution (2.5×10^{-20} liter) and a large range of volume measurement from to 10^{-19} to 10^{-9} liter. Second, the living material investigated requires minimal preparation or staining—a usually laborious process with other techniques. Third, it has a fast response time and can rapidly estimate cell volume changes, thus allowing dynamic

changes of the order of milliseconds, as well as over hours. This includes an ability to assess complex rearrangement of cell shape and changes in cell volume. Fourth, it can provide, in parallel with cell volume changes, highly local structural information and regional membrane changes in volume, for example, dendritic processes. All the foregoing lend themselves to, perhaps, the most important aspect. The SICM can monitor changes in the cells after experimental interventions. As examples of this, we have tried to choose several cell types to represent a small spectrum of cells involved in volume regulation. The A6 cell line shows, as part of its original function, aspects of volume regulation. The heart cells demonstrate volume changes under osmotic stress: a situation relevant to cell responses in ischemia and reperfusion in the whole heart. The neoplastic breast cancer cells show surface membrane changes related to abnormal growth under possible cell signal stimulation. Finally, the scanning ion conductance microscope can include additional cellular imaging with multifunctional probes or other types of real-time microscopy, making it a potentially formidable research tool.

Ventricular myocytes were kindly provided by Peter H. Sugden (National Heart and Lung Institute Division, Imperial College School of Medicine, London, U.K.). Our work is supported by the British Heart Foundation, the Office of Naval Research, University of London Central Research Fund, the Wellcome Trust, the Cancer Research Campaign, and the Garfield Weston Trust.

REFERENCES

Alvarez-Leefmans, F. J., S. M. Gamiño, and L. Reuss. 1992. Cell volume changes upon sodium pump inhibition in *Helix aspersa* neurones. *J. Physiol.* 458:603–619.

Alvarez-Leefmans, F. J., H. Cruzblanca, S. M. Gamiño, J. Altamirano, A. Nani, and L. Reuss. 1994. Transmembrane ion movements elicited by sodium pump inhibition in *Helix aspersa* neurons. *J Neurophysiol.* 71:1787–1796.

Arkawa, H., K. Umemura, and A. Ikai. 1992. Protein images obtained by STM, AFM and TEM. *Nature.* 358:171–173.

Bard, A. J., F. F. Fan, D. T. Pierce, P. R. Unwin, D. O. Wipf, and F. Zhou. 1991. Chemical imaging of surfaces with the scanning electrochemical microscope. *Science.* 254:68–74.

Basilico, C., and D. Moscatelli. 1992. The FGF family of growth factors and oncogenes. *Adv. Cancer Res.* 59:115–165.

Binnig, G., C. F. Quate, and C. Gerber. 1986. Atomic force microscope. *Phys. Rev. Lett.* 56:930–933.

Binnig, G., and H. Rohrer. 1982. Scanning tunnelling microscopy. *Helv. Phys. Acta.* 55:726–735.

Crowe, W. E., J. Altamirano, L. Huerto, F. J. Alvarez-Leefmans. 1995. Volume changes in single N1E-115 neuroblastoma cells measured with a fluorescent probe. *Neuroscience.* 69:283–296.

Errington, R. J., M. D. Fricker, J. L. Wood, A. C. Hall, and N. S. White. 1997. Four-dimensional imaging of living chondrocytes in cartilage using confocal microscopy: a pragmatic approach. *Am. J. Physiol.* 272: C1040–C1051.

Farinas, J., M. Kneen, M. Moore, and A. S. Verkman. 1997. Plasma membrane water permeability of cultured cells and epithelia measured by light microscopy with spatial filtering. *J. Gen. Physiol.* 110:283–296.

Guilak, F. 1994. Volume and surface area measurement of viable chondrocytes in situ using geometric modelling of serial confocal sections. *J. Microsc.* 173:245–256.

Hallows, K. R., C. H. Packman, and P. A. Knauf. 1991. Acute cell volume changes in anisotonic media affect F-actin content of HL-60 cells. *Am. J. Physiol.* 261:C1154–C1161.

Hansma, H. G., and J. H. Hoh. 1994. Biomolecular imaging with the atomic force microscope. *Annu. Rev. Biophys. Struct.* 23:115–139.

Hansma, P. K., B. Drake, O. Marti, S. A. C. Gould, and C. B. Prater. 1989. The scanning ion-conductance microscope. *Science.* 243:641–643.

Henderson, E., P. G. Haydon, and D. S. Sakaguchi. 1992. Actin filament dynamics in living glial cells imaged by atomic force microscopy. *Science.* 257:1944–1946.

Hoffmann, E. K., L. O. Simonsen, and I. H. Lambert. 1993. Cell volume regulation: intracellular transmission. *Advan. Compar. Env. Physiol.* 14:187–248.

Iwaki, K., V. P. Sukhatme, H. E. Shubeita, and K. R. Chein. 1990. α and β-adrenergic stimulation induces distinct patterns of immediate early gene expression in neonatal rat myocardial cells. *J Biol. Chem* 265: 13809–13817.

Johnston, C. L., H. Cox, J. J. Gomm, and R. C. Coombes. 1995. bFGF and aFGF induce membrane ruffling in breast cancer cells but not in normal breast epithelial cells. *Biochem. J.* 306:609–616.

Kawahara, K., M. Onodera, and Y. Fukuda. 1994. A simple method for continuous measurement of cell height during a volume change in a single A6 cell. *Jpn. J. Physiol.* 44:411–419.

Korchev, Y. E., C. L. Bashford, M. Milovanovic, I. Vodyanoy, and M. J. Lab. 1997a. Scanning ion conductance microscopy of living cells. *Biophys. J.* 73:653–658.

Korchev, Y. E., M. Milovanovic, C. L. Bashford, D. C. Bennett, E. V. Sviderskaya, I. Vodyanoy, and M. J. Lab. 1997b. A specialised scanning ion-conductance microscope for imaging of living cells. *J. Microsc.* 188:17–23.

Lee, G. M. 1989. Measurement of volume injected into individual cells by quantitative fluorescence microscopy. *J. Cell Sci.* 94:443–447.

McManus, M., J. Fischbarg, A. Sun, S. Hebert, and K. Strange. 1993. Laser light-scattering system for studying cell volume regulation and membrane transport processes. *Am. J. Physiol.* 265:C562–C570.

Meinild, A., D. A. Klaerke, D. D. Loo, E. M. Wright, and T. Zeuthen. 1998. The human Na^+-glucose cotransporter is a molecular water pump. *J. Physiol..* 508:15–21.

Nakahari, T., M. Murakami, H. Yoshida, M. Miyamoto, Y. Sohma, and Y. Imai. 1990. Decrease in rat submandibular acinar cell volume during ACh stimulation. *Am. J. Physiol.* 258:G878–886.

Radmacher, M., R. W. Tillmann, M. Fritz, and H. E. Gaub. 1992. From molecules to cells: imaging soft samples with the atomic force microscope. *Science.* 257:1900–1905.

Schoenenberger, C. A., and J. H. Hoh. 1994. Slow cellular dynamics in MDCK and R5 cells monitored by time-lapse atomic force microscopy. *Biophys. J.* 67:929–936.

Saito, T., N. A. Hartell, H. Muguruma, S. Hotta, S. Sasaki, M. Ito, and I. Karube. 1998. Light dose and time dependency of photodynamic cell membrane damage. *Photochem. Photobiol.* 68:745–748.

Sariban-Sohraby, S., M. Burg, and R. J. Turner. 1984. Aldosterone-stimulated sodium uptake by apical membrane vesicles from A6 cells. *J. Biol. Chem.* 259:11221–11225.

Swanson, J. A., M. Lee, and P. E. Knapp. 1991. Cellular dimensions affecting the nucleocytoplasmic volume ratio. *J. Cell Biol.* 115:941–948.

Valverde, M. A., T. D. Bond, S. P. Hardy, J. C. Taylor, C. F. Higgins, J. Altamirano, and F. J. Alvarez-Leefmans. 1996. The multidrug resistance P-glycoprotein modulates cell regulatory volume decrease. *EMBO J.* 15:4460–4468.

Zhu, Q., P. Tekola, J. P. Baak, and J. A. Beliën. 1994. Measurement by confocal laser scanning microscopy of the volume of epidermal nuclei in thick skin sections. *Anal. Quant.. Cytol. Histol.* 16:145–152.